

Cite this article as: Wang Boya, Luo Yumeng, Liu Rui, et al. Effect of Oxygen Content on Dynamic Deformation Behavior of Pure Titanium[J]. Rare Metal Materials and Engineering, 2024, 53(06): 1517-1522.
DOI: 10.12442/j.issn.1002-185X.20230553.

ARTICLE

Effect of Oxygen Content on Dynamic Deformation Behavior of Pure Titanium

Wang Boya^{1,2,3}, Luo Yumeng^{1,2}, Liu Rui^{1,2}, Song Xiaoyun^{1,2}, Yu Yang^{1,2}, Ye Wenjun^{1,2}, Hui Songxiao^{1,2,4}

¹ State Key Laboratory of Nonferrous Metals and Processes, China GRINM Group Co., Ltd, Beijing 100088, China; ² GRIMAT Engineering Institute Co., Ltd, Beijing 101407, China; ³ General Research Institute for Nonferrous Metals, Beijing 100088, China; ⁴ GRINM (Guangdong) Institute for Advanced Materials and Technology, Foshan 528051, China

Abstract: The deformation behavior of pure Ti, Ti-0.2wt% O, and Ti-0.4wt% O polycrystals under high strain rate was investigated by quasi-in-situ EBSD and SEM observation. Results show that under dynamic compressive deformation of 5% strain, the twinning behavior in pure Ti is very active, the twins in most grains are activated, and multiple twin variants appear in half of the grains. However, the slip trace analysis shows that the slip systems are activated in only 50% grains. With the increase in oxygen content, the proportion of twins and the twin area ratio are decreased, and multiple slips and cross slip are activated in the meantime. XRD analysis reveals that the solute oxygen atoms cause the lattice distortion and increase the c/a ratio in α -Ti, which is beneficial to the dislocation slip. The active dislocation slip inhibits the twin nucleation, and the oxygen atoms can pin dislocations to hinder the expansion of twinning boundaries. Thus, the twinning behavior is no longer active. In addition, the dynamic yield strength of pure Ti increases by about 390 MPa for every 0.2wt% increase in oxygen content. This solution hardening phenomenon mainly originates from the lattice distortion, and it is also influenced by the pinned dislocations and the jogs resulting from multiple slips and cross slip.

Key words: pure titanium; oxygen content; deformation mechanism; quasi-in-situ; high strain rate

Titanium and titanium alloys have great potential in the impact protection applications due to their low density and excellent dynamic mechanical properties^[1-4]. Therefore, deformation behavior of titanium under high strain rates has received widespread attention.

Alloying elements are important influence factors on the plastic deformation behavior of metals. Thus, in order to analyze the dynamic deformation of titanium, the effect of solutes, such as Al and V, on dynamic deformation of Ti polycrystal has been investigated^[5-8]. As the commonest interstitial element in titanium alloys, oxygen has a significant impact on material properties, but it is uncontrollable in low-cost titanium alloys^[9-10]. Besides, its effect on dynamic deformation behavior is rarely studied.

The effect of oxygen on the quasi-static deformation behavior of Ti polycrystal has been investigated, but the research mainly focuses on the slip^[11-14]. Twinning phenomenon in Ti polycrystal is promoted at high strain rates^[15], so the difference

between quasi-static and dynamic deformation mechanisms is huge^[16]. Therefore, the effect of oxygen on the dynamic deformation behavior of Ti polycrystal should be further studied.

In this research, the effect of oxygen content on the dynamic mechanical properties and deformation mechanisms of Ti polycrystals was investigated. The dynamic compressive mechanical properties of pure Ti, Ti-0.2wt% O, and Ti-0.4wt% O polycrystals were tested by split Hopkinson pressure bar (SHPB), and the twinning and slip behavior of these materials were investigated by quasi-in-situ electron backscattered diffraction (EBSD) and scanning electron microscope (SEM) analysis of the slip trace.

1 Experiment

The materials in this research were pure Ti, Ti-0.2wt% O (Ti-0.2O) alloy, and Ti-0.4wt% O (Ti-0.4O) alloy, and their chemical composition is shown in Table 1. All materials were

Received date: September 05, 2023

Corresponding author: Hui Songxiao, Ph. D., Professor, GRINM (Guangdong) Institute for Advanced Materials and Technology, Foshan 528051, P. R. China, E-mail: huix@grinm.com

Copyright © 2024, Northwest Institute for Nonferrous Metal Research. Published by Science Press. All rights reserved.

Table 1 Chemical composition of experiment materials (wt%)

Material	O	C	H	N	Fe	Ti
Pure Ti	0.03	0.0038		0.0016		
Ti-0.2O	0.22	0.0042	<0.0020	0.0017	<0.0050	Bal.
Ti-0.4O	0.41	0.0062		0.0018		

rolled into sheets with 8 mm in thickness and then annealed to obtain similar equiaxed structure. Fig. 1a–1c show EBSD inverse pole figures (IPFs) of the pure Ti, Ti-0.2O, and Ti-0.4O polycrystals, respectively. Statistically, the grain sizes of pure Ti, Ti-0.2O, and Ti-0.4O polycrystals are 124, 154, and 110 μm , as shown in Fig. 1d–1f, respectively. Fig. 1g–1i show the $\{0001\}$ pole figures (PFs) of the pure Ti, Ti-0.2O, and Ti-0.4O polycrystals, respectively. It can be seen that the texture with the highest intensity is the c -axis shifted by about 25° from normal direction (ND) to transverse direction (TD).

The lattice parameters were obtained by X-ray diffraction (XRD) analysis. The dynamic compression test was conducted through SHPB (the bar diameter is 14.5 mm). The schematic diagram of typical SHPB apparatus is shown in Fig. 2a. The apparatus pushes the striker by adjusting the air pressure of the gas gun, so the striker strikes the incident bar at a certain speed, producing an elastic stress wave which travels through the incident bar. When the stress wave reaches the specimen, part of the stress wave is reflected back to the incident bar due

to the difference in wave impedance between the bar and the specimen. Other parts are loaded on the specimen and then transmitted into the transmitted bar. The incident wave ε_i , reflected wave ε_r , and transmitted wave ε_t were recorded by the strain gages attached to the incident and transmitted bars. Then, the stress (σ), strain (ε), and strain rate ($\dot{\varepsilon}$) of the Ti polycrystals could be calculated by Eq.(1–3), respectively, as follows:

$$\sigma = E_b \frac{A_b}{A_s} \varepsilon_t \quad (1)$$

$$\varepsilon = -\frac{2C_b}{L_s} \int_0^t \varepsilon_r dt \quad (2)$$

$$\dot{\varepsilon} = -\frac{2C_b}{L_s} \varepsilon_r \quad (3)$$

where E_b is the Young's modulus of the bars; A_b and A_s are the initial cross-sectional area of the bar and the specimen, respectively; C_b is the elastic wave velocity in the bar; L_s is the initial length of the specimen.

The specimen used in the dynamic compression tests was cylinders of $\phi 5 \text{ mm} \times 5 \text{ mm}$, whose axial direction, i. e., loading direction (LD), was along the rolling direction (RD). The test was conducted at room temperature and the strain rate was controlled at 4000 s^{-1} .

The schematic diagrams of the specimen used for quasi-in-situ observation are shown in Fig. 2b and 2c^[5,17]. The dimen-

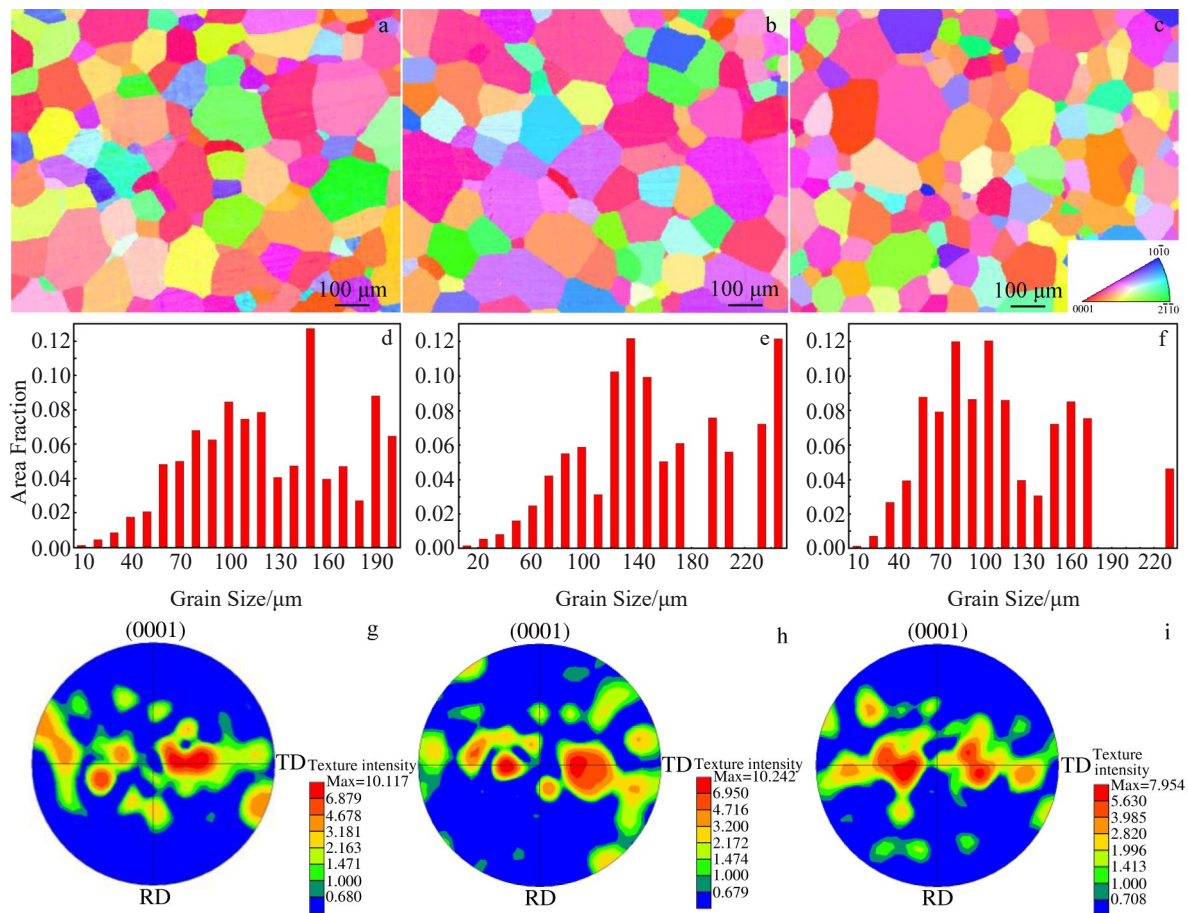


Fig.1 EBSD IPFs (a–c), grain size distributions (d–f), and $\{0001\}$ PFs (g–i) of pure Ti (a, d, g), Ti-0.2O (b, e, h), and Ti-0.4O (c, f, i) polycrystals

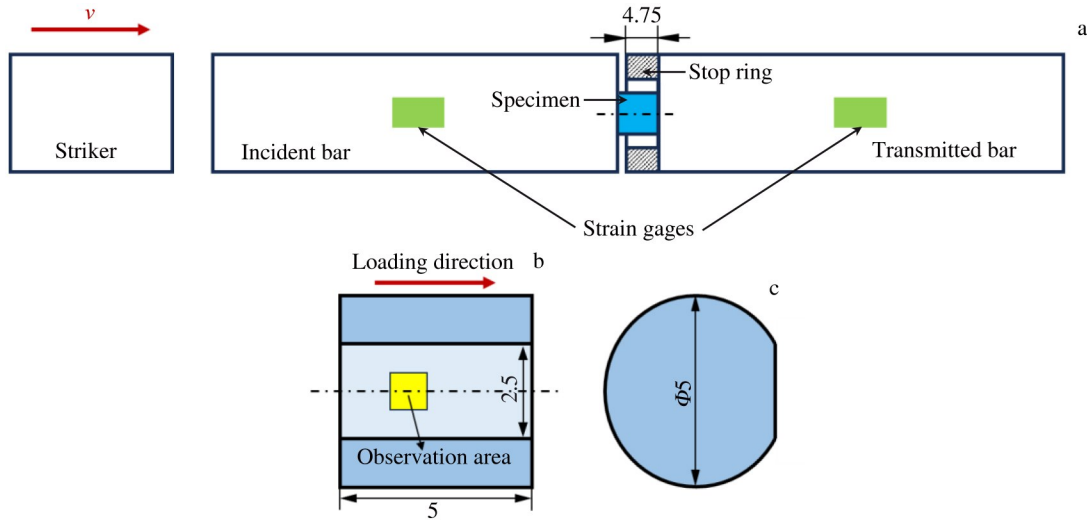


Fig.2 Schematic diagram of SHPB apparatus (a); schematic diagrams of specimen for quasi-in-situ observation in front view (b) and left view (c)

sion of the observation surface was 2.5 mm \times 5 mm. The cylinder side was machined for observation, and the surface was ground by sandpaper and then electrolytically polished. The observation area on this surface was marked by laser and observed by EBSD. This specimen was then loaded using SHPB with the same LD and strain rate for the dynamic compression test, and the strain was controlled as 5% by a stop ring with 4.75 mm in height. This deformed specimen was observed by EBSD and SEM, and then it was compared with the undeformed specimen. The twinning and slip trace analyses were also conducted.

2 Results and Discussion

2.1 Lattice parameter

Fig. 3a shows XRD patterns of pure Ti, Ti-0.2O, and Ti-0.4O polycrystals. All peaks are calibrated as close-packed hexagonal (hcp)-Ti. However, with the O addition, all peaks have a slight shift to the lower angle region, as shown in Fig. 3b. The higher the O content, the more obvious the angle shift, which indicates that the O addition increases the lattice parameter of the Ti polycrystals. Fig. 3c shows the lattice parameters of three materials obtained from XRD results. It is

found that the c/a ratio of Ti polycrystals increases from 1.587 to 1.593 with the increase in oxygen content. This phenomenon confirms that oxygen atoms are solutes in α -Ti, which causes lattice distortion. It is known that the oxygen is interstitial solute and located at hcp octahedral site^[10]. Meanwhile, with the increase in oxygen content, different peaks have different intensities, which may be caused by the subtle differences in the textures of three materials.

2.2 Dynamic mechanical properties

Fig. 4a shows the incident, reflected, and transmitted waves of Ti polycrystals in the dynamic compression tests. Different heights of the incident waves originate from different striker speeds, which can control strain rate of materials with different strengths. As a result, the reflected waves of three materials are essentially coincident. According to Eq.(3), three materials have the same strain rates, whereas different heights of the transmitted waves are related to the difference in strength of three materials.

Fig. 4b shows the true stress-true strain curves of three materials at room temperature and strain rate of 4000 s⁻¹. It is found that the dynamic yield strength of pure Ti is about 227 MPa and increases by about 390 MPa for every 0.2wt%

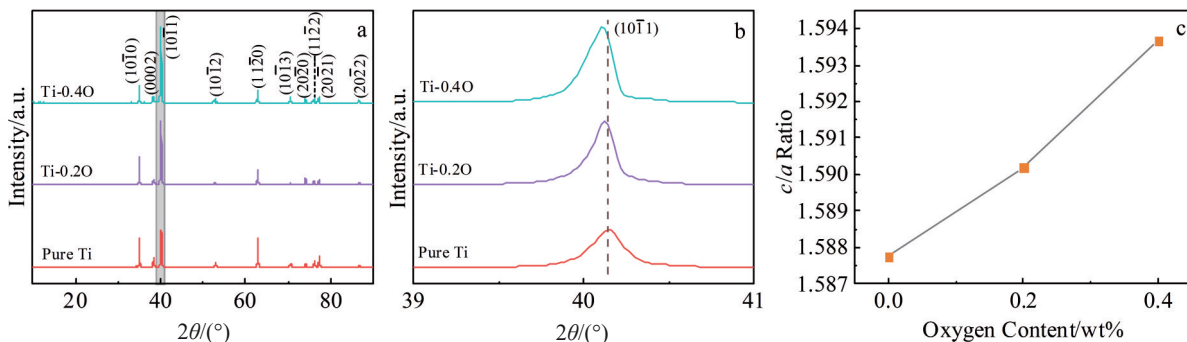


Fig.3 XRD patterns (a), localized enlargement of (10 $\bar{1}$ 1) peaks of XRD patterns (b), and c/a ratios (c) of pure Ti, Ti-0.2O, and Ti-0.4O polycrystals

increase in oxygen content. This is mainly because the critical resolved shear stress of deformation mechanisms related in the yield phase is elevated by the lattice distortion effect, which demonstrates the solution hardening caused by oxygen addition.

In addition, all three polycrystals have good plasticity, and no fracture occurs. The sharp decrease in strength is caused by the unloading process.

2.3 Deformation mechanisms

2.3.1 Pure Ti polycrystal

The change of deformation mechanisms is the fundamental reason for the improvement of mechanical properties. Therefore, the dynamic deformation mechanisms of Ti polycrystals with different oxygen contents are analyzed.

IPFs of the observation area of pure Ti polycrystal before and after dynamic compressive deformation with 5% strain are shown in Fig.5a–5b, respectively. It can be seen that twins appear in 75% grains, and there are twin lamellae along different directions in grain 1, 2, 4, and 7 in Fig.5b, indicating that multiple twin variants are activated in these grains. According to statistics, it is found that all twins have misorientation angle of 86° with the matrix and are determined as $\{10\bar{1}2\}$ twins. Furthermore, up to three kinds of twin variants are activated in the grain 2 and 4, and the total area fraction of twins is about 10%. The twinning systems are very active in pure Ti polycrystal.

Significant twin-twin interactions can be observed in the grain 2. Within the blue rectangle area in Fig.5b, the second twin variant is activated from the twin boundary of the first variant, indicating that the stress-concentrated twin boundary can promote the nucleation of other twin variants. Meanwhile, as shown in the red rectangle area in Fig.5b, when the twin variants encounter other twin variants in the growth process, mutual hindrance occurs, thereby impeding the expansion. Therefore, different twin variants can both promote and hinder the growth of other twin variants.

Fig.5c shows SEM microstructure of grain 2 in Fig.5b. The twin lamellae along different directions as well as a set of parallel slip lines can be observed. The slip lines are shallow and unclear. Similar slip lines can also be observed in grain 5, 6, and 8, indicating that only 50% grains have activated slip systems. Thus, the slip systems are not very active in pure Ti polycrystal.

Briefly, in the pure Ti polycrystal, the twin systems are much more active than the slip systems, revealing that twinning is the dominant deformation mechanism at high strain rate.

2.3.2 Ti-0.2O polycrystal

Fig. 6a–6b show IPFs of Ti-0.2O polycrystals before and after dynamic compressive deformation with 5% strain, respectively. In Fig.6b, twins can only be observed in the grain 1, 5, and 8. Only grain 1 and grain 8 have two twin variants. Both the number of grains with the twins and the kinds of twin var-

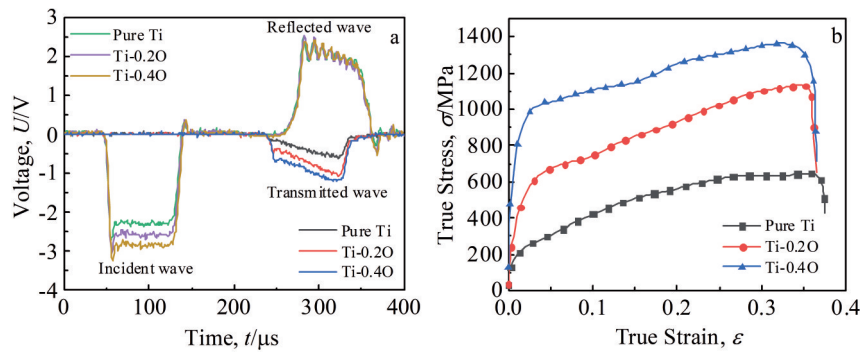


Fig.4 Incident, reflected, and transmitted waves (a) and dynamic compressive true stress-true strain curves (b) of pure Ti, Ti-0.2O, and Ti-0.4O polycrystals

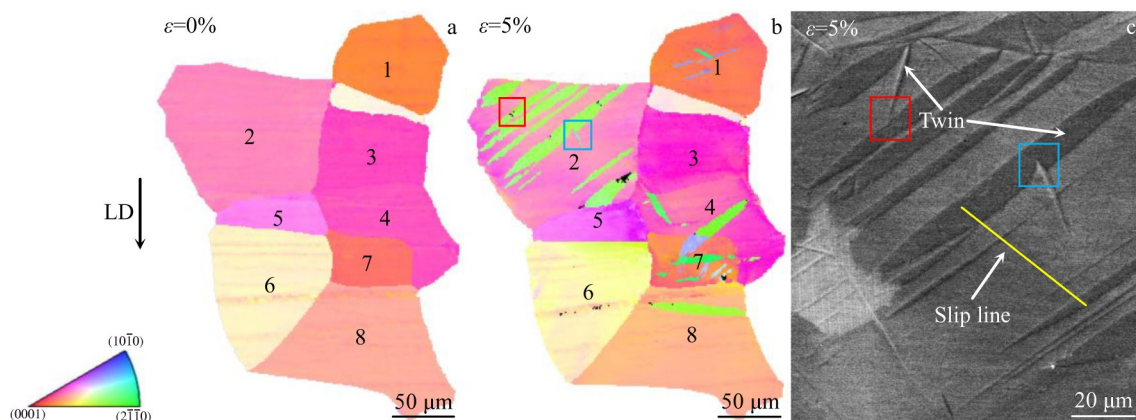


Fig.5 IPFs of observation area of pure Ti polycrystal before (a) and after (b) dynamic compressive deformation with 5% strain; SEM microstructure of grain 2 in Fig.5b (c)

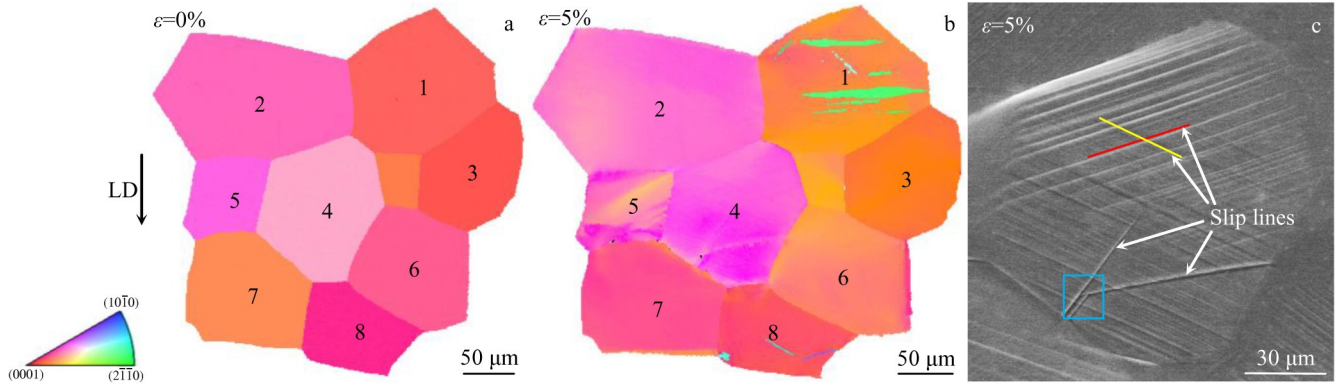


Fig.6 IPFs of observation area of Ti-0.2O polycrystal before (a) and after (b) dynamic compressive deformation with 5% strain; SEM microstructure of grain 4 in Fig.6b (c)

variants are less than those of the pure Ti polycrystal. According to statistics, it is found that the twins are still $\{10\bar{1}2\}$ twins, but the total area fraction of twins is only 2%. Overall, the activity of twin systems in Ti-0.2O polycrystal is significantly lower than that of pure Ti polycrystal. Meanwhile, the reduction in twin variants reduces the twin-twin interactions.

In the deformed Ti-0.2O polycrystal, slip lines can be observed in every grain, and the cross slip lines can also be observed in some grains, as indicated by the red and yellow lines in Fig.6c. Slip lines are the intersection lines between the slip planes and the specimen surface. The dislocations slipping on the same slip plane will form a set of parallel slip lines, and the dislocations slipping on different slip planes will form slip lines along different directions. Therefore, the crossed slip lines appear in the same grain, indicating that dislocations slip on multiple slip planes, i.e., the occurrence of multiple slips. Meanwhile, some folded slip lines can be observed in the blue rectangle area in Fig.6c, indicating the occurrence of cross-slip. This is because once the propagation of dislocations is hindered in the slip plane, they may slip into other slip planes to continue their propagation. This process may occur repeatedly, forming the folded curved slip lines. In addition, all slip lines are deeper and clearer than those in the pure Ti polycrystal, indicating that the slip behavior is more

active in Ti-0.2O polycrystal.

Compared with those in the pure Ti polycrystal, the twin systems are less active and the slip systems are more active in the Ti-0.2O polycrystal. Thus, both slip and twinning are important deformation mechanisms.

2.3.3 Ti-0.4O polycrystal

According to Fig.7b, no twins appear in the deformed Ti-0.4O polycrystal. Additionally, the slip lines are deeper and denser, and much more crossed slip lines can be observed in Fig.7c. These slip lines indicate that multiple slips are very active in the Ti-0.4O polycrystal, and slip is the dominant deformation mechanism.

In addition, more folded slip lines can be observed in the yellow rectangle area in Fig.7c, indicating that the cross-slip is also very active in Ti-0.4O polycrystal.

Comparing the deformation mechanisms in three polycrystals, it is found that the twinning gradually becomes inactive with the increase in oxygen content. At the same time, the slip activity is enhanced, and the multiple slip and cross-slip occur.

This is because with the increase in oxygen content, the c/a ratio of Ti polycrystal is increased and becomes closer to that of hcp crystals with the perfect stacking. These phenomena all result in the more active slip systems, and therefore the multiple slips occur. Slip gradually replaces twinning as the

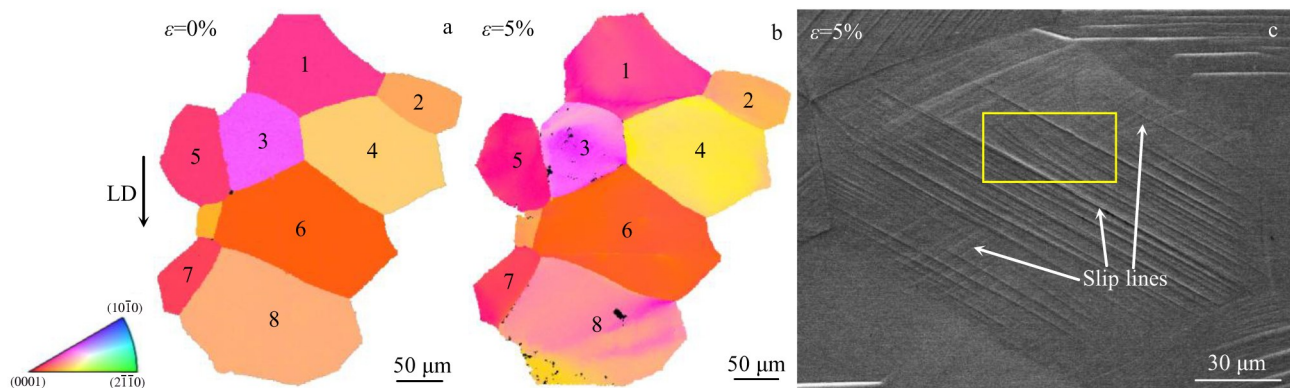


Fig.7 IPFs of observation area of Ti-0.4O polycrystal before (a) and after (b) dynamic compressive deformation with 5% strain; SEM microstructure of grain 4 in Fig.7b (c)

dominant deformation mechanism. At the same time, the interstitial solute oxygen atoms pin the dislocations. Therefore, the deformation resistance improves; some hindered dislocations slip to other slip planes for easier slip, resulting in the cross-slip; the pinned dislocations can further hinder the expansion of twin boundaries. Multiple slips and cross-slip cause many jogs, and the pinned dislocations as well as the jogs contribute to the solution hardening effect.

3 Conclusions

1) The yield strength of Ti polycrystal increases by about 390 MPa for every 0.2wt% increase in oxygen content. Solution hardening mainly originates from the lattice distortion caused by oxygen addition.

2) At high strain rates, twinning is the main deformation mechanism in pure Ti polycrystal. However, with the increase in oxygen content, the total area fraction of twins and the kinds of twin variants are decreased. Besides, the slip systems are activated more frequently. Meanwhile, multiple slips and cross-slip occur. Slip gradually becomes the dominant deformation mechanism.

3) The change of deformation mechanism of Ti polycrystal originates from the interstitial solution of oxygen atoms. With the increase in oxygen content, c/a ratio is increased, resulting in more active slip and the occurrence of multiple slips. At the same time, oxygen atoms pin the dislocations, which hinders the dislocation slip and causes cross-slip. The active slip suppresses twinning, and the pinned dislocations prevent the expansion of twin boundaries. In addition, the pinned dislocations and the jogs caused by multiple slips and cross-slip also conduce to solution hardening effect.

References

1 Hou Hongmiao, Qin Cheng, Pan Hao et al. *Titanium Industry*

Progress[J], 2022, 39(5): 1 (in Chinese)

- 2 Alaghmandfard R, Dharmendra C, Odeshi A G et al. *Materials Science and Engineering A*[J], 2020, 793: 139794
- 3 Li Yanxing, Zhou Zhe, Wang Lin et al. *Rare Metal Materials and Engineering*[J], 2023, 52(3): 953 (in Chinese)
- 4 Xin Shewei, Hao Fang, Zhou Wei et al. *Rare Metal Materials and Engineering*[J], 2022, 51(1): 295 (in Chinese)
- 5 Luo Y M. *IOP Conference Series: Materials Science and Engineering*[J], 2019, 585: 012017
- 6 Wang Q C, Liu R, Ye W J et al. *Materials Science Forum*[J], 2017, 898: 231
- 7 Wang Q C, Hui S X, Ye W J et al. *Rare Metals*[J], 2018, 42: 2361
- 8 Liu Qinghua, Hui Songxiao, Ye Wenjun et al. *Rare Metal Materials and Engineering*[J], 2013, 42(7): 1464 (in Chinese)
- 9 Wasz M, Brotzen F, McLellan R et al. *International Materials Reviews*[J], 1996, 41(1): 1
- 10 Yu Q, Qi L, Tsuru T et al. *Science*[J], 2015, 347(6222): 635
- 11 Ren J Q, Wang Q, Lu X F et al. *Materials Science and Engineering A*[J], 2018, 731: 530
- 12 Chaari N, Rodney D, Clouet E. *Scripta Materialia*[J], 2019, 162: 200
- 13 Barkia B, Couzinié J P, Lartigue-Korinek S et al. *Materials Science and Engineering A*[J], 2017, 703: 331
- 14 Kale C, Garg P, Bazehhour B G et al. *Acta Materialia*[J], 2019, 176: 19
- 15 Xu F, Zhang X, Ni H et al. *Materials Science and Engineering A*[J], 2012, 541: 190
- 16 Dai L, Song W. *International Journal of Plasticity*[J], 2022, 154: 103281
- 17 Luo Y M, Guo W Q, Wang B Y et al. *Crystals*[J], 2022, 12(5): 677

氧含量对纯钛动态变形行为的影响

王博雅^{1,2,3}, 骆雨萌^{1,2}, 刘睿^{1,2}, 宋晓云^{1,2}, 于洋^{1,2}, 叶文君^{1,2}, 惠松骁^{1,2,4}

(1. 中国有研科技集团有限公司 有色金属材料制备加工国家重点实验室, 北京 100088)

(2. 有研工程技术研究院有限公司, 北京 101407)

(3. 北京有色金属研究总院, 北京 100088)

(4. 有研(广东)新材料技术研究院, 广东 佛山 528051)

摘要: 通过准原位EBSD和SEM观察研究了纯钛、Ti-0.2% O和Ti-0.4% O(质量分数)多晶体在高应变速率下的变形行为。结果表明: 在5%应变的动态压缩变形下, 纯钛中的孪生行为非常活跃, 多数晶粒内的孪生系被激活, 且半数晶粒中出现多种孪生变体; 而滑移迹线分析表明, 仅有50%的晶粒内开动了滑移系。随着氧含量的增加, 孪生晶粒比例及孪晶面积占比均呈下降趋势, 同时发生多滑移与交滑移。XRD分析表明, 溶质氧原子导致晶格畸变, 提高了 α -Ti的 c/a , 有利于位错滑移。活跃的位错滑移行为抑制了孪晶的形成, 并且氧原子钉扎位错也会阻碍孪晶界的扩展, 导致孪生行为不再活跃。此外, 氧含量每增加0.2%(质量分数), 纯钛的动态屈服强度就能增加约390 MPa。这种固溶强化现象主要源于晶格畸变, 也受到被钉扎位错及多滑移和交滑移产生的割阶影响。

关键词: 纯钛; 氧含量; 变形机制; 准原位; 高应变速率

作者简介: 王博雅, 女, 1997年生, 博士生, 北京有色金属研究总院, 北京 100088, E-mail: boya0314@hotmail.com